

Finite Element Modeling Under Stress by the Nonlinearity of a Material Ferromagnetic

M. Mohammedi

Electrical Department, Faculty of Science Engineering
University of Skikda, Skikda, Algeria
mohammedimoufid@yahoo.fr

T. Bahi

Electrical Department, Faculty of Science Engineering
University of Annaba, Annaba, Algeria
tbahi@hotmail.com

Y. Soufi

Electrical Department, Faculty of Science Engineering
University of Tébessa, Tébessa, Algeria
y_soufi@yahoo.fr

Abstract: In this paper, we present a numerical procedure allow of analyzing dynamic hysteresis in axial-symmetric problems. The ferromagnetic hysteresis is described by Jiles-Atherton model. This model is integrated in finite element method (FEM) in order to resolve magneto-dynamic problems. The interface between the Jiles-Atherton model and the finite element magnetic vector potential formulation is introduced through the fixed-point iterative technique. The simulation results obtained are intended to give an explanation and understanding of nonlinear behavior of ferromagnetic material and their effect on the magnitude of the electromagnetic system.

Key words: hysteresis, Finite element, Preisach model, Jiles–Atherton model.

1. Introduction.

The complexity of the geometry and the nonlinear behavior of the electrotechnical systems make the formulation of the model more complex to solve. The finite element method and the simulation techniques have rapidly spread with the development of the computer. Therefore the digital computer calculation of the performance of devices, including nonlinear magnetic materials, requires the use of the curves of the hysteresis magnetic. The magnetic characteristic must be accurately introduced into this method [1]-[2]. The development of an accurate analytical or numerical method which accounts for magnetic hysteresis is needed for many applications in which the magnetic field influences the performance of the component. The work presented in this paper develops such a method by coupling the finite element equations, and the Jiles-Atherton dynamic hysteresis model. In this work we use the Jiles-Atherton state model to represent hysteresis and magnetic saturation effects and the finite elements method to account for two-dimensional geometric effects. The two approaches are combined with the method of the fixed point used for the resolution the nonlinear problem. It

consists in repeatedly solving the problem until the convergence of the solution by integrating the calculation of the hysteresis loop. The process of the fixed point applied to the finite elements for the formulation in potential vector seems very natural, one takes as variable point fixes the magnetization since it is known at the initial moment. A general transient model is obtained that can be used to calculate the local magnetic field state along with the current variable. Finally, simulation results confirm the validity of the approach.

2. Dynamic model of Jiles-Atherton

In order to describe the magnetic proprieties of material, the Jiles-Atherton model is used in this effort because it provides a relatively simple, yet reasonably accurate, expression for magnetization [3]-[4]-[5]. It is based on the theory of ferromagnetic hysteresis, rather than only on mathematical arguments or experimental curve fitting. The magnetization is represented as the sum of three types of energy, energy due to the losses by eddy current, the anormal losses and the losses by hysteresis. The latter are includes implicitly.

Firstly, the energy due to the losses by eddy current is determined as:

$$\frac{dW_{fc}}{dt} = \frac{e^2}{2\rho\beta} \left(\frac{dB}{dt}\right)^2 = \frac{\mu_0^2 e^2}{2\rho\beta} \left(\frac{dM}{dt}\right)^2 \quad (1)$$

Secondly, the anormal losses are:

$$\frac{dW_A}{dt} = \left[\frac{G \cdot e \cdot w \cdot H_0}{\rho} \right]^{1/2} \left(\frac{dB}{dt}\right)^{1/2} \quad (2)$$

Finally, the total energy is given by:

$$\mu_0 \int M_{an} dH_e = \mu_0 \int M dH_e + \mu_0 k \delta (1-c) \int dM_{irr} \quad (3)$$

So, the magnetization is represented by the following equation:

$$\left(\frac{\mu_0 e^2}{2\rho\beta} \cdot \frac{dH}{dt}\right) \left(\frac{dM}{dh}\right)^2 + \left(\frac{\mu_0 G e w H_0}{\rho}\right)^{1/2} \left(\frac{dH}{dt}\right)^{1/2} \left(\frac{dM}{dH}\right)^{1/2} + \left(k\delta - \alpha \left(M_{an} - M_{irr} + k\delta \cdot \frac{dM_{an}}{dH_e}\right)\right) \left(\frac{dM}{dH}\right) - \left(M_{an} - M + k\delta \frac{dM_{an}}{dH_e}\right) = 0 \quad (4)$$

α : factor that accounts for inter domain coupling;

k : coefficient accounting for the pinning energy;

ρ : resistivity of material.;

e : thickness of the sheet;

w : weight of the sheet;

G, β : Constants depending on material;

μ_0 : permeability of air ($\mu_0 = 4 \cdot \pi \cdot 10^{-7} H/m$);

δ : directional parameter, equal +1 or -1 for increasing or decreasing field respectively.

The anhysteretic magnetization in follows the Langevin function (5), which is a nonlinear function of the effective field (6).

$$M_{an}(H_e) = M_s \left(\coth\left(\frac{H_e}{a}\right) - \left(\frac{a}{H_e}\right) \right) \quad (5)$$

$$H_e = H + \alpha \cdot M \quad (6)$$

Where a is a normalization constant of the field H , and M_s is the saturation magnetization. The Langevin equation is applicable for isotropic materials in which the magnetization has no preferred direction.

By taking into account the preceding expressions, the result of simulation is obtained. The area of the hysteresis loop increases with increasing frequency and consequently the increase in the losses by hysteresis (see Fig.1).

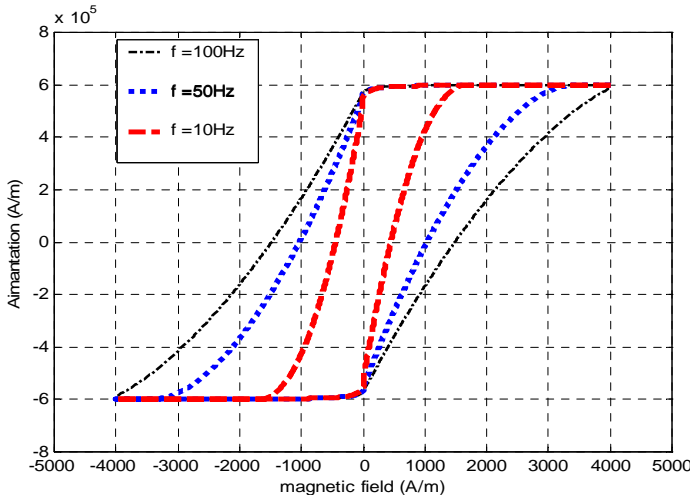


Fig.1. Effect of the frequency on the hysteresis loop.

3. Finite element code with model dynamic of hysteresis magnetic

The hysteresis model represented by (4) is included into the finite element code [6]–[7]–[8]. These code permits to resolve 2D magneto-dynamic problem expressed in terms of vector potential:

$$\sigma \cdot \frac{\partial A}{\partial t} + \text{curl} \left(\frac{1}{\mu_0} \cdot \text{curl}(A) \right) = J_s + \text{curl}(M) \quad (7)$$

The constitutive relationship is:

$$B = \mu_0 \cdot (H + M(H)) \quad (8)$$

J_s : current density; σ : electric conductivity; B : flux density; M : hysteresis magnetization; H : magnetic field.

When applying Galerkin's weighted residual approach to (7) we obtain the following integral form:

$$\iint_{\Omega} \omega_i \cdot \left[\text{curl}(\text{curl}A) + \mu_0 \cdot \sigma \left(\frac{\partial A}{\partial t} \right) \right] d\Omega = \iint_{\Omega} \omega_i \cdot \mu_0 \cdot \left(\vec{J}_s + \text{curl}M \right) d\Omega \quad (9)$$

ω_i : Ponduration function.

With the following linear approximation for the vector potential:

$$A = \sum \omega_i \cdot A_i \quad (10)$$

Then, we obtain the following algebraic form:

$$[K] \cdot \left[\frac{\partial A}{\partial t} \right] + [M] \cdot [A] = [F] + [G(A)] \quad (11)$$

$$\left\{ \begin{array}{l} K_{ij} = \iint_{\Omega} \sigma \mu_0 \omega_i \omega_j d\Omega \\ M_{ij} = \iint_{\Omega} \left(\frac{\partial \omega_i}{\partial x} \cdot \frac{\partial \omega_j}{\partial x} + \frac{\partial \omega_i}{\partial y} \cdot \frac{\partial \omega_j}{\partial y} \right) \\ F_i = \iint_{\Omega} \omega_i \cdot \mu_0 \cdot J_s \cdot d\Omega \\ G_i = \iint_{\Omega} \mu_0 \cdot \left(\frac{\partial \omega_i}{\partial x} \cdot M_y + \frac{\partial \omega_i}{\partial y} \cdot M_x \right) \end{array} \right. \quad (12)$$

The proposed algorithm whose details are shown in figure 2.

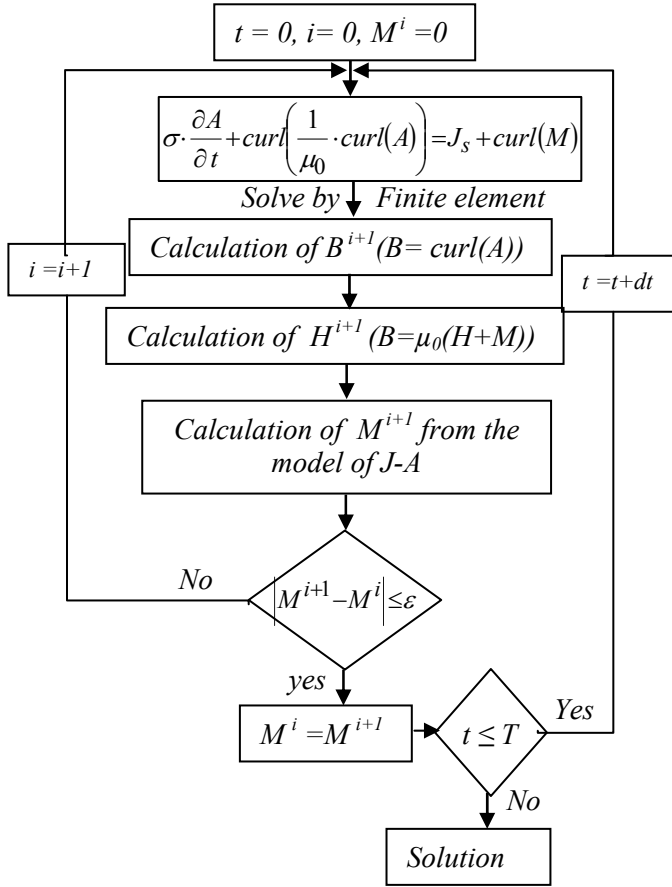


Fig.2. Proposed algorithm.

4. Test problem modelling and simulating

The proposed algorithm whose details are shown in figure 2 is applied to an heating induction system. This latter is represented by a cylindrical ferromagnetic material surrounded by a conductive coil (see Fig.3). The magnetic characteristics of the ferromagnetic material are $k = 1$, $H_c = 1000 \text{ A/m}$, $H_s = 5000 \text{ A/m}$. The current density in the coil is $J_s = 10^6 \text{ A/m}^2$.

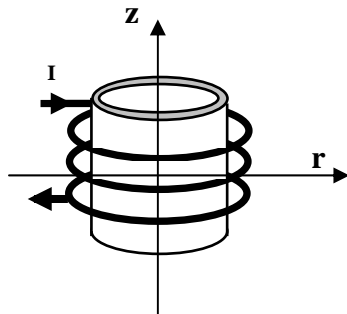


Fig 3. The studied system.

5. Simulation results

The numerical computations were performed using computer programs developed under Matlab environment. The results from simulation allow us to have the impact of magnetic hysteresis on the magnetic sizes such as the magnetic potential vector A . In figure 4, we present only the quarter of the system to reduce the number of mesh elements, we shows the inductor, the load (ferromagnetic material) and the surrounding air. The boundary conditions are taken according to Derichlet ($A=0$) and Neuman ($\frac{\partial A}{\partial N} = 0$).

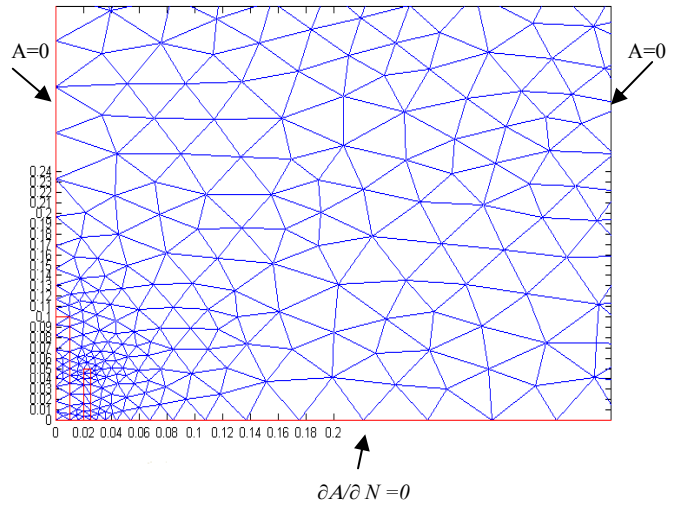


Fig.4. Grid of the domain with boundary conditions.

The figure 5 represents the equipotentials of potential vector A , which to justify the boundary conditions shown in figure 4.

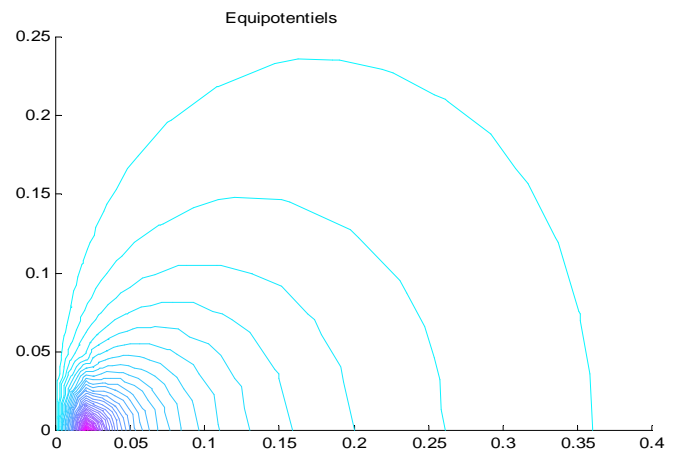


Fig .5. Equipotentials of potential vector A .

The figure.6 represents the evolutions of the magnetic potential vector with and without hysteresis for each node located on axis r (for $t=5.10^{-5}$, $t=2.5.10^{-5}$), one notice the value of A is inversely proportional to the distance from the node compared to the inductor (current source).

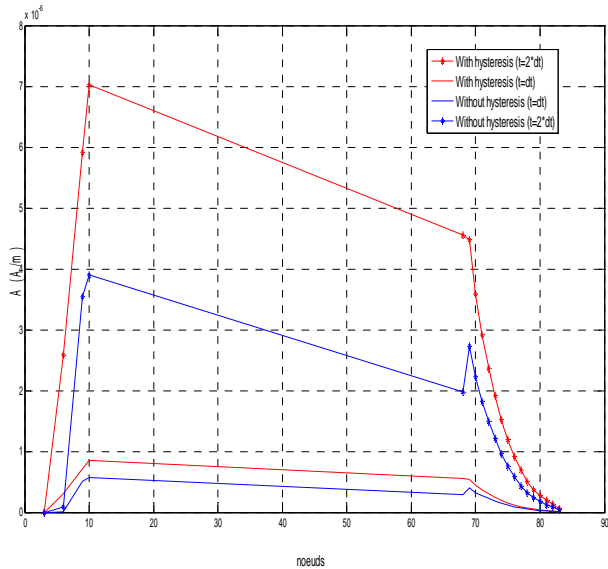


Fig.6. Magnetic vector potential for each nodes along the axis r .

The evolutions of the magnetic potential vector with and without hysteresis according to axis r (for $t=5.10^{-5}$, $t=dt=2.5.10^{-5}$) are represents in the figure 7. By incrementing the time, the current density and consequently the vector potential increases.

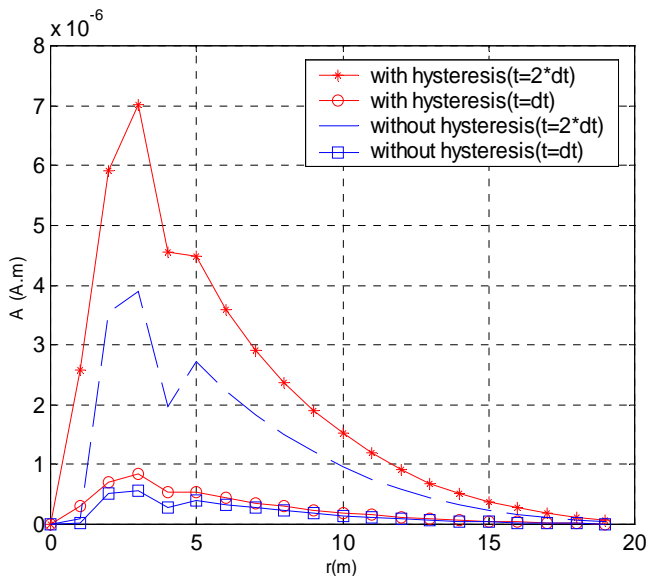


Fig.7. Evolutions of the magnetic potential with r .

The nonlinear behavior of ferromagnetic material is the nonlinear characteristic of the magnetization as a function of magnetic field (Fig.8.a) or susceptibility depends on the magnetic field (Fig.8.b). When the element is more near to the source, the magnetization increases more rapidly and its saturation value is high.

In view of the evolution of the magnetization represented by the figure 8.a, we note that the corresponding susceptibility (Fig.8.b) increases to its maximum and begins to decrease when the magnetization is near to the saturation, eventually

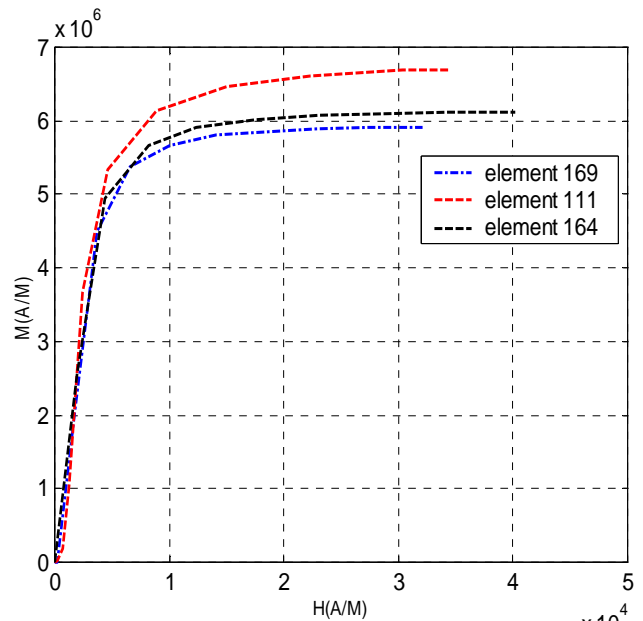


Fig.8.a. Magnetization.

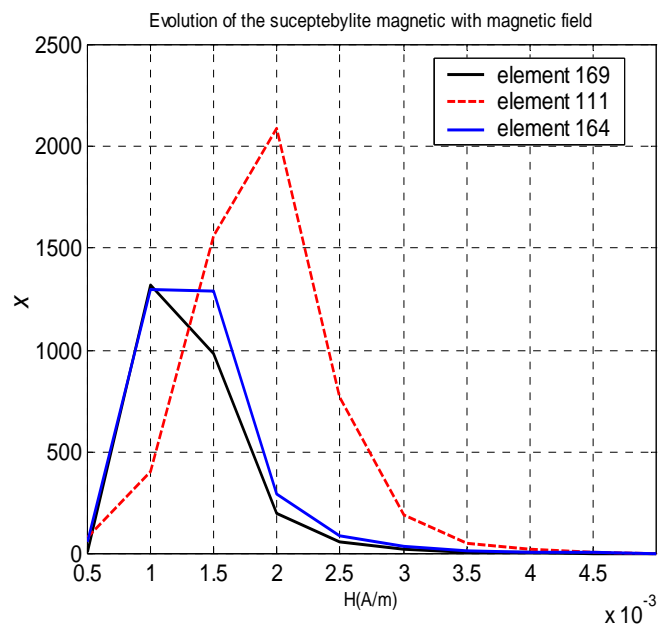


Fig.8.b. Magnetic susceptibility.

Fig.8. Nonlinear behavior of ferromagnetic material.

The figure 9, shows the spatial distribution of saturation induction (B_s) for each element of the ferromagnetic material.

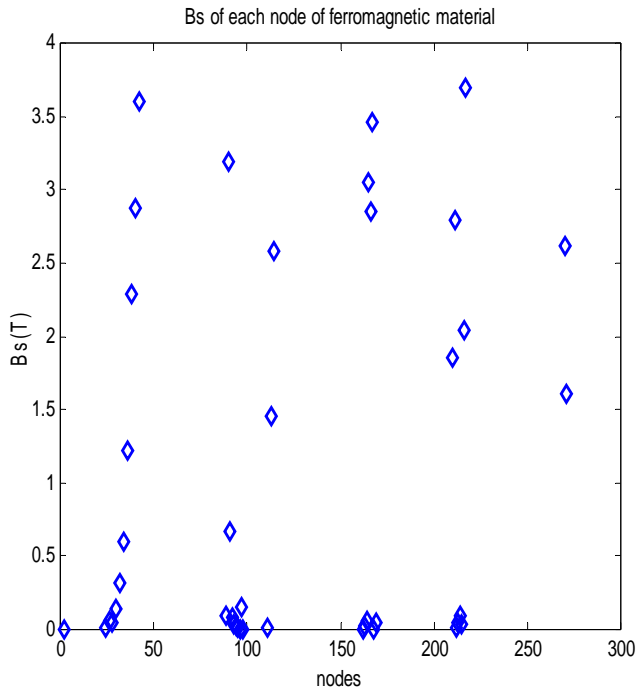


Fig.9. Spatial distribution of B_s .

The figure 10, shows the spatial distribution of saturation induction (B_s) for each element of the ferromagnetic material and for different values of frequency.

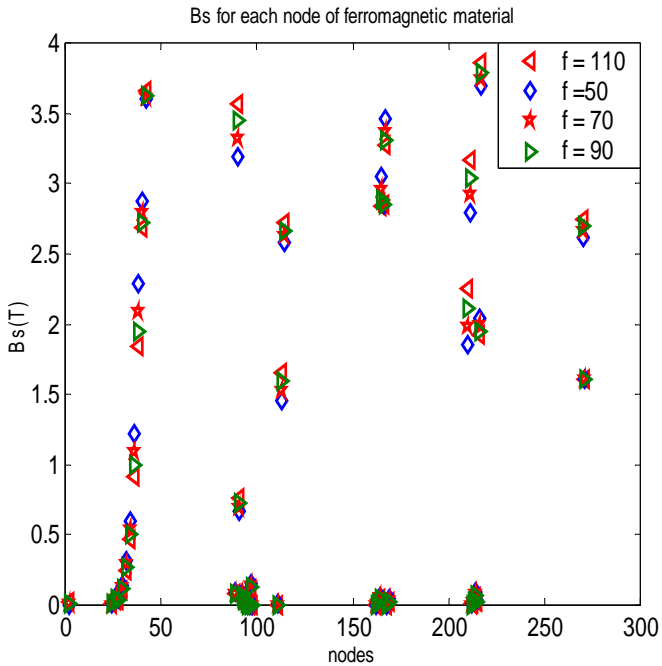


Fig.10. Spatial distribution of B_s for different values of frequency.

The figure 11 enables us to clearly see the impact of the dynamic model of magnetic hysteresis on the induced currents, when the frequency increases the induced currents increase.

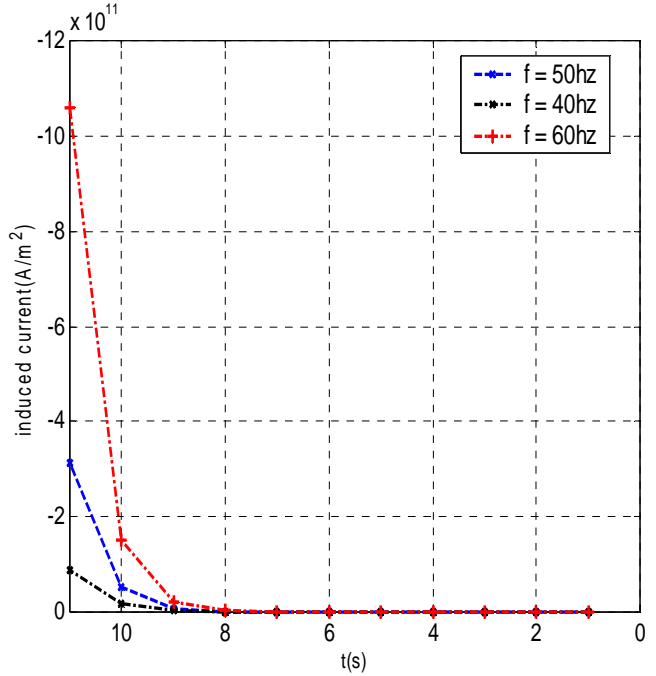


Fig .11. Evolution of the induced currents .

6. Conclusion

The purpose of our work is to make an accurate model which takes into account the non linearity of the behavior of ferromagnetic material, used in the construction of the majority of the electro technical systems.

Our application is an induction heating, we illustrate the effect of the dynamic behavior of the model of magnetic hysteresis, for three values of the frequency, on the induced currents, when the frequency increases the induced currents increase. Then it is important to take into account the phenomenon of hysteresis in the electrotechnical systems modeling.

References

1. H. L. Toms, R. G. Colclaser, Jr., Fellow, M. P. Krefta, "Two-Dimensional finite element magnetic modelling for scalar hysteresis effects," IEEE Trans. on Magn., vol. 37, no. 2, march 2001.
2. E. Dlala, J. Saitz, A. Arkkio, "Inverted and forward Preisach models for numerical analysis of electromagnetic field problems," IEEE Trans. on Magn., vol. 42, no. 8, august 2006.
3. F. Liorzou, B. Phelps, and D. L. Atherton, "Macroscopic Models of Magnetization," IEEE Trans. on Magn, vol. 36, no. 2, march 2000.
4. D. C. Jiles and D. L. Atherton, "Theory of ferromagnetic hysteresis," Journal of Magnetism and Magnetic Materials, vol. 61, pp. 48–60, 1986.
5. D. C. Jiles, J. B. Thoelke, and M. K. Devine, "Numerical Determination of Hysteresis Parameters for the Modeling of Magnetic Property Using the Theory of Ferromagnetic Hysteresis," IEEE Transaction on Magnetism, vol. 28, pp. 27–35, Jan. 1992.
6. T. Chevalier, G. Meunier, A. Kedous-Lebouc, and B. Cornut "Numerical Computation of the Dynamic Behavior of Magnetic Material Considering Magnetic Diffusion and Hysteresis," IEEE Trans on Magn, vol. 36, no. 4, july 2000.
7. Y. Ouled Amor, M. Féliachi, H. Mohellebi, "A new convergence procedure for the finite element computing associated to Preisach hysteresis model," IEEE Trans. on Magn., vol. 36, no. 4, july 2000.
8. P. I. Koltermann, J. P. A. Bastos, N. Sadowski, N. J. Batistela, A. Kost, L. Jänicke, K. Miethner, "Nonlinear magnetic field model by FEM taking into account hysteresis characteristics with M - B variables," IEEE Trans. on Magn., vol. 38, no. 2, march 2002.